

Cardiac fat adipocytes: An optimized protocol for isolation of ready-to-use mature adipocytes from human pericardial adipose tissue

Stefano Quarta^a, Giuseppe Santarpino^{b,c,d}, Maria Annunziata Carluccio^a, Nadia Calabriso^a, Francesco Cardetta^e, Laura Siracusa^f, Tonia Strano^f, Ilaria Palamà^g, Gabriella Leccese^g, Francesco Visioli^h, Marika Massaro^{a,*}

^a Institute of Clinical Physiology (IFC), National Research Council (CNR), 73100 Lecce, Italy

^b Department of Clinical and Experimental Medicine, Magna Graecia University of Catanzaro, Italy

^c Department of Cardiac Surgery, Città di Lecce Hospital, GVM Care&Research, Lecce, Italy

^d Department of Cardiac Surgery, Paracelsus Medical University, Nuremberg, Germany

^e Department of Cardiac Surgery, University "Campus Biomedico", Rome, Italy

^f Institute of Biomolecular Chemistry (ICB), National Research Council (CNR), Catania section, Via Paolo Gaifami 18, 95126 Catania, Italy

^g Institute Nanotechnology Institute, CNR-NANOTEC, 73100 Lecce, Italy

^h Department of Molecular Medicine, University of Padova, Italy

ARTICLE INFO

Keywords:

Cardiac adipose tissue

Adipocytes

Inflammation

Fatty acid analysis

Adipocyte-endothelium interaction

ABSTRACT

A better understanding of the pathophysiology of cardiac fat depots is crucial to describe their role in the development of cardiovascular diseases. To this end, we have developed a method to isolate mature fat cells from the pericardial adipose tissue (PAT), the most accessible cardiac fat depot during cardiac surgery. Using enzymatic isolation, we were able to successfully obtain mature fat cells together with the corresponding cells of the stromal vascular fraction (SVF). We subjected the PAT adipocytes to thorough morphological and molecular characterization, including detailed fatty acid profiling, and simultaneously investigated their reactivity to external stimuli. Our approach resulted in highly purified fat cells with sustained viability for up to 72 h after explantation. Remarkably, these adipocytes responded to multiple challenges, including pro-inflammatory and metabolic stimuli, indicating their potential to trigger a pro-inflammatory response and modulate endothelial cell behavior. Furthermore, we have created conditions to maintain whole PAT in culture and preserve their viability and reactivity to external stimuli. The efficiency of cell recovery combined with minimal dedifferentiation underscores the promise for future applications as a personalized tool for screening and assessing individual patient responses to drugs and supplements or nutraceuticals.

1. Introduction

The adipose tissue is no longer considered as a simple connective tissue that stores calories in lipid droplets. Rather, it is now acknowledged as a remarkably intricate organ, remarkably influencing physiology and pathophysiology [1]. The adipose tissue is distributed

throughout the body, forming accumulations identified as specific depots including, but not limited to, visceral, mammary, dermal, and bone marrow adipose depots [2]. Notably, certain specialized adipose depots are intricately linked to the associated anatomical structures, thereby expressing tissue- and organ-specific functionalities. A representative case is cardiac fat, a subtype of visceral fat that has garnered significant

Abbreviations: EAT, epicardial adipose tissue; PAT, pericardial adipose tissue; SVF, stromal vascular fraction; CCM, cell-conditioned medium; OCM, organ-conditioned medium (OCM); FSC, forward scatter; SSC, side scatter; APN, adiponectin; PPAR- γ , Peroxisome proliferator-activated receptor γ ; PLIN-1, Perilipin-1; MMP-9, Matrix metalloproteinase-9; VCAM-1, Vascular Cell Adhesion Molecule 1; COX-2, Cyclooxygenase-2; MCP-1, Monocyte chemoattractant protein-1; HMEC-1, human dermal microvascular endothelial cells-1; 7-AAD, 7-Aminoactinomycin D; FAMES, fatty acid methyl esters; FID, flame ionization detector; GC-MS, gas-chromatography-mass spectrometry.

* Corresponding author at: Institute of Clinical Physiology of the National Research Council (IFC-CNR), Via Monteroni, Lecce, Italy.

E-mail addresses: stefanoquarta@cnr.it (S. Quarta), santarpino@unicz.it (G. Santarpino), maria.carluccio@cnr.it (M.A. Carluccio), nadia.calabriso@cnr.it (N. Calabriso), f.cardetta@unicampus.it (F. Cardetta), laura.siracusa@icb.cnr.it (L. Siracusa), tonia.strano@cnr.it (T. Strano), ilaria.palama@nanotec.cnr.it (I. Palamà), gabriella.leccese@nanotec.cnr.it (G. Leccese), francesco.visioli@unipd.it (F. Visioli), marika.massaro@cnr.it (M. Massaro).

<https://doi.org/10.1016/j.jmcc.2024.08.006>

Received 3 May 2024; Received in revised form 23 August 2024; Accepted 27 August 2024

Available online 28 August 2024

0022-2828/© 2024 Published by Elsevier Ltd.

attention from the global cardiovascular community over the last twenty years. Cardiac fat is regarded as a potential contributor to the pathophysiology of coronary atherosclerosis and cardiac function, in turn stimulating extensive instrumental clinical research and interest in its implications [3]. Cardiac fat resides in three distinct regions recognized as pericardial, epicardial, and intramyocardial adipose tissues with different embryological origin and vascularization [4]. Pericardial Adipose Tissue (PAT) comprises fat deposits located between the visceral and parietal pericardium [5]. The Epicardial Adipose Tissue (EAT) is positioned posterior to the PAT and is situated between the visceral layer of the pericardium and the heart, without any fascia barrier from the myocardium [6]. This lack of barrier allows EAT to directly envelop the myocardium and coronary vessels, providing a housing for the ganglia of the cardiac nervous system and vascular plexi [6]. Formerly overlooked as a predominantly mechanical element of the heart, the characterization of cardiac adipose tissues has deeply evolved over time. In addition to its role as a cushion and structural support that protects the coronary arteries from mechanical stress and torsion, recent understanding has revealed new metabolic and pathogenic functions [6]. As a metabolically active tissue with paracrine and exocrine capabilities, EAT actively contributes to the homeostasis of the cardiovascular system serving as a store for triglycerides and playing a key role in energy production in the heart muscle [7]. Nevertheless, prolonged and excessive energy intake, mirroring the dynamics observed in other adipose depots, may trigger a pathological expansion of both PAT and EAT, resulting in significant dysregulation of cellular functions [8]. As weight increases and adipose tissue expands, adipose cells undergo a shift towards pro-inflammatory phenotypes. This transition is accompanied by an enhanced recruitment of pro-inflammatory T-cells and M1 macrophages, occurring at the expense of anti-inflammatory M2 macrophages [9] overall stigmata of coronary atherosclerosis [10]. Correspondently, the expansion in both EAT [11] and PAT [12] volumes has been correlated with heightened atherosclerotic risk. While some authors have attributed a more pronounced pro-atherosclerotic role to EAT [13–15], more recent evidence has confirmed that increased PAT volume is also associated with coronary and extracoronary atherosclerotic plaque development and inflammation, suggesting that PAT also plays a possible pathogenic role [16–18]. Enhancing our comprehension of the pathophysiology of cardiac fat depots would significantly aid in defining the role of cardiac fats in the development of cardiovascular disease. Moreover, it would pave the way for the future development of innovative therapeutic strategies. To achieve this goal, the best practice approach involves the availability of suitable cellular models that accurately represent each cardiac fat depot and respond sensitively to external manipulations. In pursuit of this objective, we developed a method to isolate mature adipocytes from PAT, which is the most readily accessible cardiac fat depot during cardiac surgery interventions. The adipose cells from PAT underwent comprehensive morphological and molecular characterization, while simultaneously evaluating their response to external stimuli. Through this process, we established and characterized a novel cardiac adipose model, which can serve as a valuable resource for investigating the physio-pathological aspects of obesity-related atherosclerosis and for assessing the effectiveness of potential new therapeutic interventions.

2. Material and methods

2.1. Chemicals

Type 2 collagenase was obtained from Worthington Biochemicals (Lakewood, NJ, USA). 7-Aminoactinomycin D (7-AAD) was obtained from BioLegend (Uithoorn, Netherlands), while Nile Red and CD90 (Thy-1)-PE monoclonal antibody were from Invitrogen (distributed by Thermo Fisher Inc.). Unless otherwise indicated, all other reagents were purchased from Sigma-Aldrich.

2.2. PAT sample collection and processing

Our studies were conducted in accordance with the ethical guidelines of the Declaration of Helsinki [19] and approved by the Ethics Committee of Lecce (Italy, N. 21, 02072018). All patients gave written informed consent before surgery. Human PAT samples were collected from eight patients (of both sexes and on standard therapy with statins and antihypertensive drugs) undergoing elective cardiac surgery (coronary artery bypass grafting – CABG - or heart valve surgery) at the Città di Lecce Hospital (Lecce, Italy). The PAT samples (approx. 3 cm³) were taken ventral to the pericardium before the start of extracorporeal circulation (Fig. 1A). The samples were stored dry at 4 °C in sterile containers and utilized within three hours of being obtained from the explant. Longer storage times resulted in a reduction in cell viability. After rapid transportation to the research laboratory, the adipose tissues were immediately processed under a biosafety level 2 cabinet. Sample were weighed and minced with sterile blades, taking care to remove visible clots and cauterized parts. They were then rinsed with phosphate buffered saline (PBS) without calcium and magnesium to remove excess blood. The tissue pieces prepared in this manner were used for two main purposes: setting up PAT organ cultures (section 2.3) and isolating mature adipocytes and stromal vascular fraction (SVF) cells (section 2.4).

2.3. PAT organ culture setup

For the setup of organ cultures, PAT samples were further cut into pieces of approximately 25–30 mg each, transferred to multi-well plates and maintained in 500 µL of completed medium (DMEM/F12 supplemented with 10% foetal bovine serum (FBS) or 0.1% bovine serum albumin (BSA), 100 mg/ml streptomycin and 100 IU/ml penicillin) /100 mg of tissue, ensuring that the pieces were fully immersed in the medium (Fig. 2). Cultures were untreated or treated with 10 ng/mL tumor necrosis factor(TNF)-α and maintained at 37 °C in a humidified incubator at 37 °C with 95% air and 5% CO₂. At the end of the incubation period, PAT pieces were broken and homogenised in PureZOL™ RNA Isolation Reagent (BioRad) using sterile pestles. We used 500 µL of TRIzol reagent for 100 mg of tissue.

2.4. Mature adipocyte and SVF cell collection

The pieces obtained in Section 2.3 were placed in sterile 50-mL tubes and then enzymatically digested by adding 2.5 mL of 1 mg/mL collagenase/0.1% BSA in DMEM/F12 preheated at 37 °C for every 1 mg of adipose tissue. The solution was allowed to preliminary equilibrate by incubating it in a humidified incubator at 37 °C with 95% air and 5% CO₂ for 15 min, with the lid unscrewed. After this time, the digestion process was completed by incubating the suspension at 37 °C for 30–60 min while shaking on an orbital shaker at 100 rpm. This step maximizes collagenase activity. To prevent unwanted cell degradation, the status of the digestion process was checked every five minutes (Fig. 1B). Meanwhile, a 300 µm nylon filter was assembled onto a sterile funnel, which was placed atop a sterile tube (Fig. 4A-B). Following the completion of collagenase digestion, the suspension was poured onto the nylon filter (Fig. 1E). This allowed the adipocytes and SVF to pass through the mesh of the filter while retaining undigested material and tissue debris. Subsequently, the resulting cell suspension was centrifuged at a low g (100 rpm) for 5 min at 25 °C to facilitate the flotation of the adipocytes and their separation from the SVF cells. The mature adipocytes (top layer) were then harvested using a sterile pipette (Fig. 1F) and transferred to a new tube containing 10 mL of the complete medium. The resulting suspension was subjected to further centrifugation at 100 rpm for 5 min at 25 °C to remove any remaining SVF cells and collagenase residues and the adipocytes were finally harvested for cell treatment and/or analysis. After removal of the adipocytes, the remaining cell suspension was centrifuged at 200 xg for 10 min at 25 °C to collect the SVF cells. These

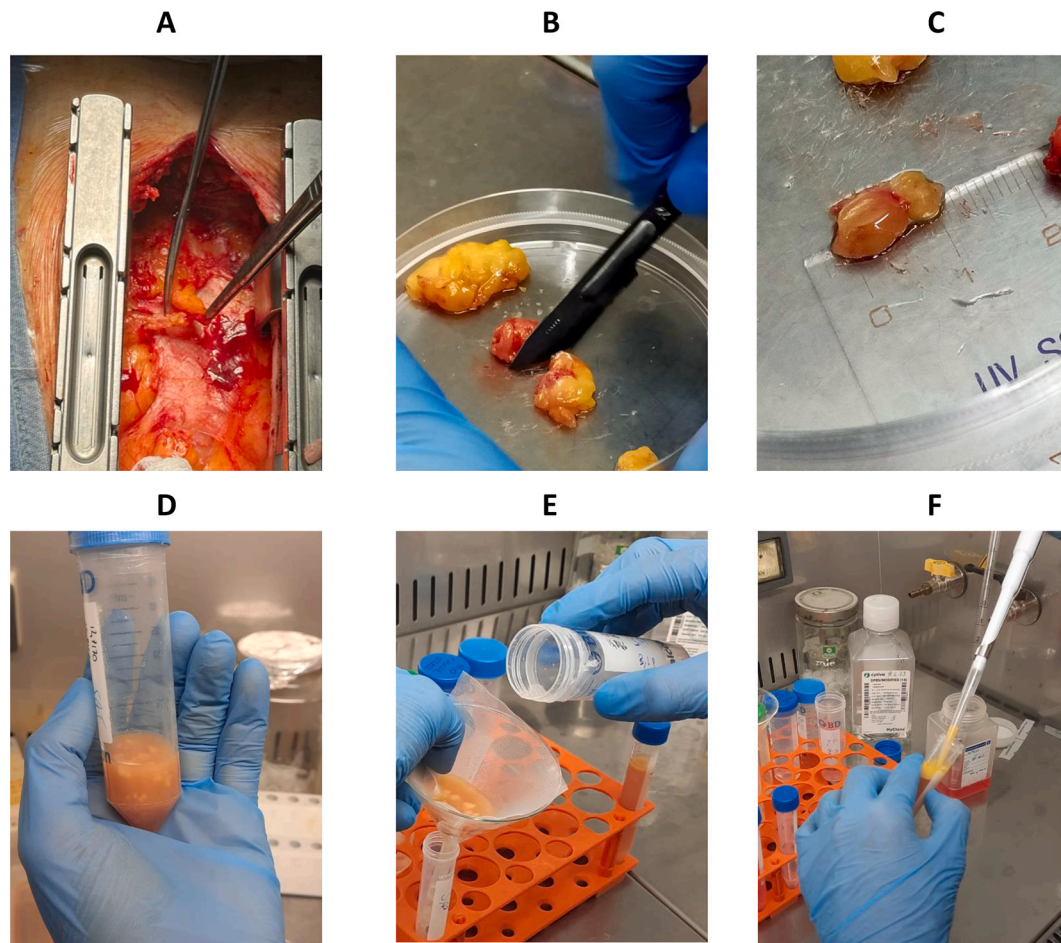


Fig. 1. Adipose tissue preparation for digestion. (A) During the surgical procedure, the first step is to carefully open the chest cavity to gain access to the heart and surrounding structures. This delicate procedure is carried out carefully to minimise damage to the surrounding tissues and organs. Once the chest is opened, the surgical team proceeds with the removal of the PAT. The harvesting of PAT is performed with extreme care and precision to ensure the integrity of the sample for subsequent analysis. (B–C) Cutting of adipose tissue in pieces of ~100 mg using sterile blades, scissors and forceps. (D) Digested adipose tissue. (E) Separation of adipocytes and SVF cells from tissue debris. (F) Tube with adipocytes after the second centrifugation.

were plated and maintained in a humidified incubator with 95% air and 5% CO₂ at 37 °C in complete medium to allow the growth of mesenchymal stem cells (MSC) from the same donors. The same procedure was used to isolate adipocytes from subcutaneous adipose tissue (SAT) samples, which were used as a comparative adipocyte source from a different fat depot.

2.5. Subculturing and treatment of PAT adipocytes

2.5.1. Cell subculturing

PAT adipocytes isolated from 1 g of tissue were suspended in 6 mL of completed medium, distributed over a cell area of 24–25 cm² and maintained as floating adipocytes (suspension cell culture) or processed into adherent cells (ceiling culture) as described by Sugihara [20]. To allow the PAT adipocytes to adhere to the culture surface, the cells harvested from 1 g of PAT were seeded into a T25 flask (with screw cap without filter) that was completely filled with complete medium. The flask was then incubated upside down for 3 days in a humidified incubator at 37 °C with 95% air and 5% CO₂. Under these conditions, the PAT adipocytes tended to float in the medium and adhere to the upper inner surface (top/ceiling surface) of the flask. After 3 days, the flask was rotated to position the cells on the lower inner surface and held in this orientation for a further day to allow the adipocytes to adhere firmly. After this time, the medium was carefully removed and the resulting adherent cells were further incubated by adding 5 ml of complete

medium.

2.5.2. Cell treatment

Floating adipocytes were stimulated at various time points (0–72 h post-isolation) with different stimuli, including 10 ng/mL TNF- α for 5 h, 100 nmol/L insulin for 30 min, and 10 μ mol/L isoproterenol for 24 h. Medium from untreated and stimulated PAT adipocytes were collected and centrifuged at 200 \times g before to be stored at –80 °C. To obtain conditioned medium from PAT adipose cells (CCM) and PAT organ culture (OCM), PAT adipocytes and PAT pieces were placed for 24 h in the upper chamber of a Transwell™ with a 0.4 μ m pore polycarbonate membrane insert. Complete medium was added to the lower chamber. After 24 h, the medium in the lower chamber was collected, centrifuged at 200 \times g and stored at –80 °C. The Transwell™ system allows us to collect only clean medium, avoiding the collection of lipid components floating in the upper chamber.

2.6. PAT adipocytes processing

After incubation, the cells were transferred to a sterile tube and centrifuged at 25 °C for 5 min at low speed. Using a sterile glass Pasteur pipette, the medium below the top layer of adipocytes was carefully aspirated. The cells were washed with warm PBS before adding the appropriate volume of lysis buffer for RNA or protein collection.

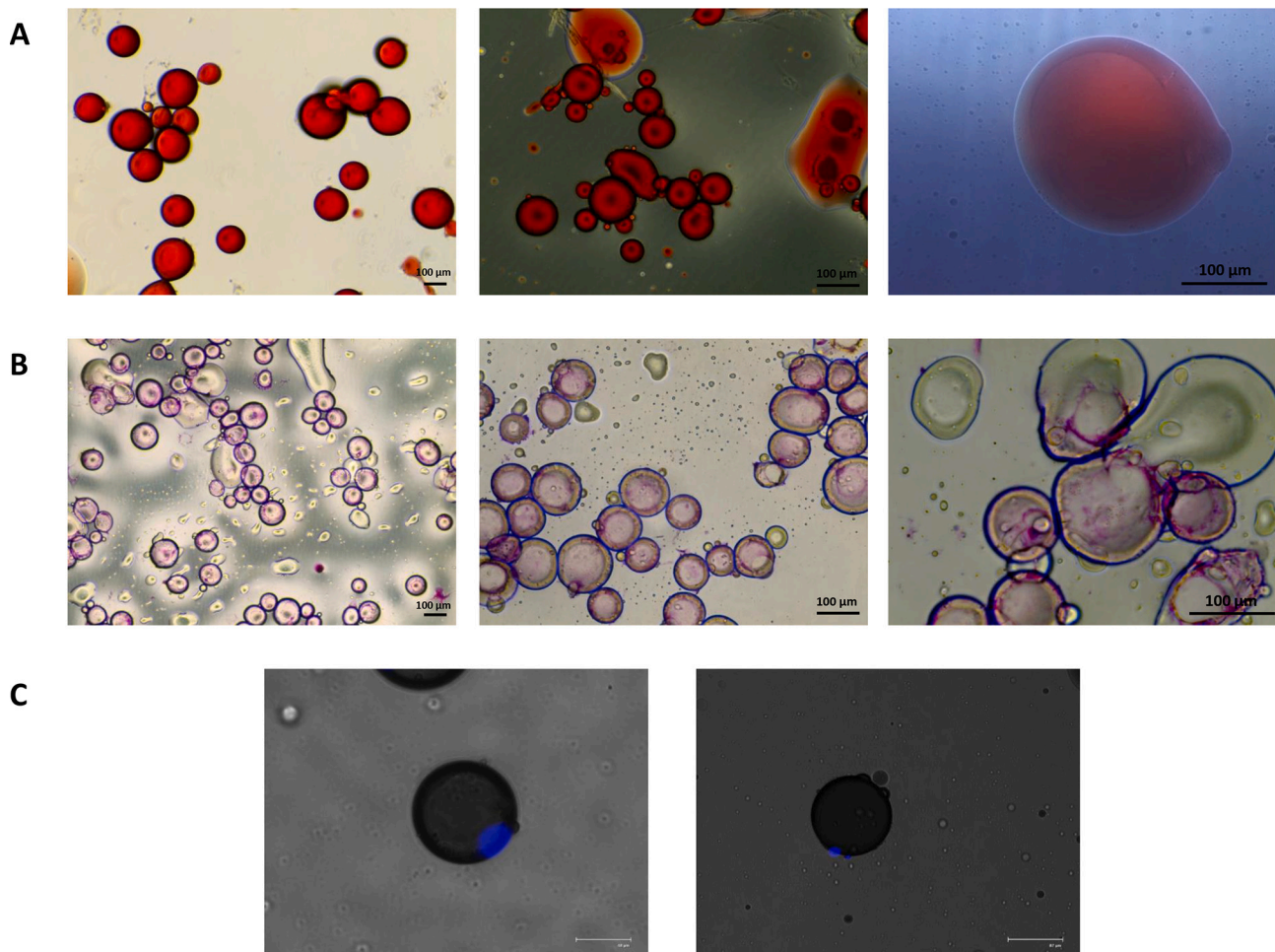


Fig. 2. Phenotypic characterization of PAT adipocytes. The isolated adipocytes were allowed to adhere to the culture surface (ceiling culture), which facilitates the staining procedure, and were stained using different methods. Images were captured at different magnifications (10–40 \times). (A) Intracellular lipids were stained with Oil Red O to (ORO). (B) Cell proteins were stained with Sulforhodamine B (SRB). (C) Cell nuclei were stained with DAPI. (For interpretation of the references to colour in this figure legend, the reader is referred to the web version of this article.)

2.7. Cell viability

Cell viability was determined using the 3-(4,5-dimethylthiazol-2-yl)-2,5-diphenyltriazolium bromide (MTT) assay, which is based on the ability of viable cells to convert MTT, a soluble tetrazolium salt, into an insoluble formazan precipitate. Briefly, both untreated and treated adipocytes isolated within 0–72 h were incubated with MTT solution (at a final concentration of 0.5 mg/mL) for 2 h. The resulting formazan products were dissolved with isopropanol, and the absorbance was measured at 595 nm using a microplate reader.

2.8. Sulforhodamine B assay

To perform the colorimetric sulforhodamine B (SRB) assay, cells adherent in T25 flasks obtained under ceiling culture conditions were used. The cells were fixed by adding 5 ml of ice-cold 10% (w/v) trichloroacetic acid for 30 min at 4 °C. After fixation, cells were washed five times with water and air-dried overnight. Subsequently, 5 ml of a 0.4% (w/v) SRB solution was added and the cells were incubated for 30 min. After the incubation period, the cells were washed four times with 1% (vol./vol.) acetic acid solution. Finally, the cells were visualized using a phase contrast microscope (10–40 \times objective) connected to a digital camera (EVOS XL Core Imaging System, Thermo Fisher Scientific).

2.9. Oil red O assay and DAPI staining

Lipid content was assessed in adherent adipocytes using oil red O (ORO) staining. First, cells were washed twice with phosphate-buffered saline (PBS) before being fixed in 10% formalin for 30 min. They were then incubated with the ORO staining solution for 1 h. After the incubation period, the unbound dye was removed by serial washing with water. The ORO-stained cells were then photographed using a phase contrast microscope (10–40 \times objective) connected to a digital camera (EVOS XL Core Imaging System, Thermo Fisher Scientific). After ORO staining, nuclei were stained with 1 μ g/ml 4',6-diamidino-2-phenylindole (DAPI) in PBS for 40 min. After washing with PBS, the DAPI-stained nuclei were visualized using an EVOS XL Cell Imaging System microscope (Thermo Fisher, Waltham, MA, USA).

2.10. Analysis of adipocytes by flow cytometry

1×10^5 events of a suspension of cells isolated from 1 g of adipose tissue and seeded in a T25 flask were stained with the vital lipophilic dyes Nile Red (1 ng/mL) [21] and analyzed by flow cytometry at CytoFLEX S (Beckman Coulter) and fluorescence read at Ex/Em = 550/640 to determine the percentage of vital isolated adipocytes. Cells were then stained with 25 ng of 7-AAD and analyzed by flow cytometry at Ex/Em = 477/678 to estimate the cell death ratio. To further characterize the isolated cellular component, MSC and adipocytes isolated from the

same donor were also stained with CD90-PE antibody. Flow cytometry data were analyzed using CytExpert analysis software (Beckman Coulter).

2.11. PAT adipocytes and mesenchymal cells fatty acid analysis

PAT adipocytes (stored at -80°C) were brought at room temperature and directly methylated in order to obtain the corresponding fatty acid methyl esters (FAMES). For the methylation, a soft procedure was applied, taken from official methods [22] and implemented in our laboratories for this specific matrix. In fact, this strategy is particularly suitable for delicate substrates that are prone to thermal degradation and/or degradation due to drastic reaction conditions. In detail, variable aliquots (approximately 100 mg) of cellular material were accurately weighed and placed in 8 mL amber vials equipped with a screw cap and a silicone septum (Agilent Technologies, Milan, Italy). Four mL of n-hexane and 1 mL of a 2 N KOH solution in methanol (11.2 g of KOH in 100 mL methanol) were then added, the heterogeneous mixture shortly stirred (2 min) at room temperature with a magnetic stirrer and then left decanting for at least 2 h until complete phase separation. The upper clean phase (hexane fraction) was then taken with a glass Pasteur pipette, treated with anhydrous sodium sulfate, filtered through Whatman No. 1 paper, placed in 2 mL GC autosampler vials and sent to analytical determinations. Methylations were performed in duplicate for each sample. For the same analyses performed on mesenchymal cells membranes, it was necessary to carry out a liquid-liquid extraction before methylation. To this end, the method proposed by Bligh and Dyer [23] was applied: aliquots (10 mg) of cell material were extracted with 1 mL of a CHCl_3 : MeOH: H_2O (1:2:0.8 v/v/v) solution, vortexed, and further extracted with 1 mL CHCl_3 : H_2O (1:1 v/v). The resulting heterogeneous mixtures were vortexed and centrifuged (10 min, 4000 rpm) in order to separate the layers. The extraction procedure was repeated three times. The organic layers were then brought together, passed over anhydrous Na_2SO_4 to eliminate any trace of residual water, and the solvents removed at reduced pressure. FAMES were analyzed in the fast mode on a Shimadzu gas chromatograph Model 17-A equipped with a flame ionization detector (FID) and an operating software Class VP Chromatography Data System version 4.3 (Shimadzu). Analytical conditions were set as follows: DB-5 MS capillary column (15 m \times 0.10 mm \times 0.10 mm), helium as carrier gas; injection in split mode (1:200), injected volume 1 μL , injector and detector temperature 250 and 280°C , respectively. Linear velocity in column 51 cm/s. The oven temperature was held at 80°C for one minute, then programmed from 80 to 280°C at $10^{\circ}\text{C}/\text{min}$ constant for 20 min. Percentages of compounds were determined from their peak areas in the GC-FID profiles. For FAMES' masses determination, gas-chromatography-mass spectrometry (GC-MS) was carried out in the fast mode on a Shimadzu GC-MS mod. GCMS-QP5050A with operating software GCMS solution version 1.02 (Shimadzu). The ionization voltage was 70 eV, the electron multiplier was set at 1000 V and the transfer line temperature was 280°C . Analytical conditions: SPB-5 Ms. (Supelco) capillary column (15 m \times 0.10 mm \times 0.10 mm), helium as carrier gas. Injection in split mode (1:96), injected volume 1 μL , injector and detector temperature 250 and 280°C , respectively. Constant linear velocity in column 50 cm/s. The oven temperature was held at 80°C for one minute, then programmed from 80 to 280°C at $10^{\circ}\text{C}/\text{min}$ constant for 20 min. Analyses were carried out in triplicate. Gas chromatographic peaks were identified based on matching of their mass spectral data with those compiled in the NIST MS 107, NIST 21, and NIST 14 libraries and comparison of the fragmentation patterns with those reported in literature.

2.12. RNA isolation and real-time quantitative polymerase chain reaction

Total RNA was isolated using TRIzol reagent (Thermo Fisher Scientific, Waltham, MA USA) according to the manufacturer's protocol. RNA was retrotranscribed using the High-Capacity cDNA Reverse

Transcription Kit (Thermo Fisher Scientific, Waltham, MA, USA) on a GeneAmp PCR System 9700 (Thermo Fisher Scientific) under the following conditions: 10 min at 25°C , 120 min at 37°C , and 5 min at 85°C . Real-time PCR (qPCR) analyses were performed using the CFX96 Touch Real-Time PCR Detection System and software (Bio-Rad, Laboratories, Segrate, Italy). All reactions were carried out in a total volume of 25 μL with 50 ng cDNA, 0.3 pmol/L of primer pair, and 12.5 μL $2 \times$ SYBR Green PCR master mix (Bio-Rad) under the following conditions: 2 min at 50°C , 10 min at 95°C , and 40 cycles of 15 s at 95°C and 1 min at 60°C . Reactions were executed in duplicate on three independent sets of RNA. Negative controls (without RNA addition) were processed under the same conditions as the experimental samples. The quantifications were performed using the comparative critical threshold method ($\Delta\Delta\text{CT}$), and β -actin gene was used as internal control for normalization. The primers used for real-time PCR analysis were listed in Table 1.

2.13. Inflammatory response on endothelial cells

As endothelial cell model, we used the human dermal microvascular endothelial cells (HMEC)-1 which were previously demonstrated to respond to different pro-inflammatory stimuli [24]. HMEC-1 were provided by Prof. E.W. Ades (Centre for Disease Control, Atlanta, GA, USA) and were cultured in MCDB-131 medium supplemented with 15% FBS, 2 mmol/L glutamine, 100 mg/mL streptomycin, 100 IU/mL penicillin, 10 ng/mL epidermal growth factor (EGF) and 0.5% hydrocortisone in a 5% CO_2 humidified atmosphere at 37°C . Human monocytic THP-1 cells were obtained from the American Tissue Culture Collection (Rockville, MD, USA) and maintained in RPMI 1640 medium supplemented with 2 mmol/L glutamine, 100 mg/mL streptomycin, 100 IU/mL penicillin, and 10% FBS in a 5% CO_2 humidified atmosphere at 37°C . To assess the pro-inflammatory activity of PAT adipocytes, confluent endothelial monolayers were exposed to OCM or CCM, both diluted 1:1 with supplemented MCDB-131. Additionally, endothelial monolayers were treated with 10 ng/mL TNF- α as a positive control.

2.13.1. Analysis of HMEC-1 gene expression

As for PAT adipocytes total RNA was isolated using TRIzol reagent according to the manufacturer's protocol and gene expression evaluated as previously described.

2.13.2. Leukocyte-Endothelial adhesion assay

Under pro-inflammatory conditions, the leukocyte-endothelium adhesion assay provides a robust system for qualitatively and quantitatively determining interactions between leukocyte-like cells and an endothelial monolayer that has been rendered dysfunctional by pro-inflammatory and/or dysmetabolic challenges [25]. Leukocyte interactions with the vascular endothelium involve a cascade of processes that culminate in the firm attachment of leukocyte-like cells to endothelial cell adhesion molecules, which are de-novo expressed on the endothelial cell surface in response to pro-inflammatory and dysmetabolic stimuli [25].

In our experimental setup to assess the pro-inflammatory activity of PAT adipocytes, confluent endothelial monolayers of HMEC-1 were exposed to either OCM or CCM, both diluted 1:1 with supplemented MCDB-131. Additionally, endothelial monolayers were treated with 10 ng/mL TNF- α as a positive control. Following this treatment, we evaluated the acquired adhesion properties of the endothelial cells by measuring how many monocytes attached to the stimulated endothelium. For this purpose, we used THP-1 cells, a well-established monocyte cell model of human origin (doi:10.21037/atm.2016.08.53). Briefly, 10^6 cells/mL of THP-1 cells were fluorescently labeled by incubation with calcein-AM (5 ng/mL) for 30–45 min, and washed with RPMI medium, while endothelial cells monolayers were fluorescently labeled by incubation with a solution of 2 $\mu\text{g}/\text{mL}$ DilC18 for 30 min before washing. Suspended THP-1 cells were then added to HMEC-1 monolayers. After 30 further minutes, nonadherent cells were removed by

Table 1
Primer sequences used for qPCR analysis.

Gene Symbol	Full Name	Forward Primer (5'-3')	Revers Primer (3'-5')	Accession Number
APN	Adiponectin	AGTCTCACATCTGGTTGGGG	CTCTCTGTGCTCTGTTCC	NM_001177800.1
PPAR-γ	Peroxisome proliferator-activated receptor γ	TGCAGGTGATCAAGAAGACG	AGTGCAACTGGAAGAAGGA	NM_005037.5
PLIN-1	Perilipin-1	TCTCGAATACACCGTGCAGAC	TGGTCCTCATGATCCTCCTC	NM_002666.5
MMP-9	Matrix metalloproteinase-9	TTGACAGCGACAAGAAGTGG	GCCATTACGTCGTCCTTAT	NM_004994.2
VCAM-1	Vascular Cell Adhesion Molecule 1	CATGGAATTGGAACCCAAAC	CCTGGCTCAAGCATGTCATA	NM_001078.3
COX-2	Cyclooxygenase-2	TGCTGTGGAGCTGTATCCTG	GAAACCCACTTCTCCACCA	NM_000963.2
MCP-1	Monocyte chemoattractant protein-1	CCCCAGTCACCTGCTGTTAT	TCCTGAACCCACTTCTGCTT	NM_002982.3
β-actin	Beta-actin	GATGAGATTGGCATGGCTTT	CACCTTCACCGTTCAGTTT	NM_001101.3

careful washing with PBS and images of HMEC-1 and adherent THP-1 cells were visualized and captured with a stereomicroscope (Nikon, Minato, Tokyo, Japan) equipped with the Nikon NIS-Elements D at 40× magnification. Finally, adherent monocytes were counted using the ImageJ program (<http://imagej.nih.gov/ij/>, accessed on 20 June 2024).

2.14. Determination of lipolysis

Lipolysis was evaluated by determining the amount of glycerol released into the culture media. To this aim, adipocytes medium aliquots were removed after isoproterenol treatment and kept at −20 °C for the subsequent measurement of glycerol concentration through a direct colorimetric procedure using a commercial kit (Cayman Chemical, Ann

Arbor, MI, USA). Briefly, the medium was incubated with glycerol kinase, glycerol phosphate oxidase, and horseradish peroxidase in the presence of a colorimetric substrate to generate a chromophore, whose intensity was read at 540 nm using a microplate reader.

2.15. Statistical analysis

The results were expressed as means ± S.D. Student's *t*-test was used to compare the means between adipocyte culture at different time points post-explantation as well as between the control group and the treated group. Multiple comparisons were conducted using one-way analysis of variance (ANOVA) followed by Bonferroni's post-hoc test. A *p* value of <0.05 was considered as statistically significant.

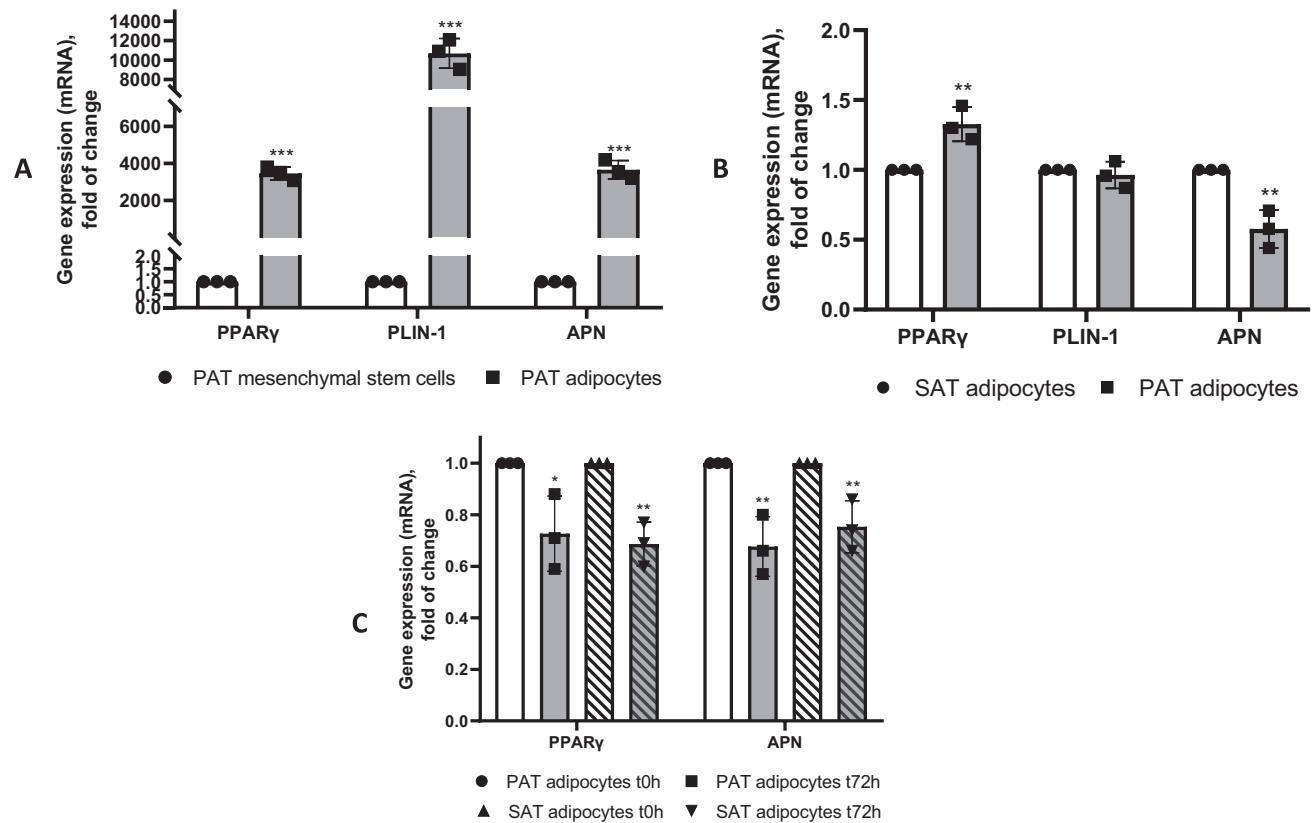


Fig. 3. PAT adipocytes express typical adipocyte genes. Total RNA was extracted from PAT and SAT adipocytes and MSC cells at different time points after isolation. The mRNA levels of PPARγ, PLIN-1 and adiponectin were measured by qPCR using specific primers and normalized to β-actin mRNA. (A) Data (mean ± S.D., n = 3 for each experimental group) are expressed as fold induction versus MSC (control). Statistical analysis was performed with Student's *t*-test. ****p* < 0.001. (B) Data (mean ± S.D., n = 3 for each experimental group) are expressed as fold induction versus SAT adipocytes. Statistical analysis was performed with Student's *t*-test. ***p* < 0.01. (C) Data (mean ± S.D., n = 3 for each experimental condition) are expressed as fold induction over isolated adipocytes at time 0 and after 72 h. Statistical analysis was performed with Student's *t*-test. **p* < 0.05; ***p* < 0.01.

3. Results

3.1. Phenotypic characterization of PAT adipocytes

The isolation method described here has produced pure populations of mature adipocytes. From 1 g of PAT tissue, we can reliably isolate approximately 2 mg of cellular protein, providing an adequate number of cells for seeding onto a growth area surface of 24 square centimeters. The PAT adipocytes maintained in culture up to five days were analyzed by various histochemical and molecular methods. First, PAT adipocytes were subjected to lipid histochemistry with Oil Red O, protein staining with sulforhodamine B and nuclear staining with DAPI. As shown in Fig. 2A, adherent PAT adipocytes after 5 days in culture exhibited typical morphological features of mature white adipocytes: a spherical shape and the presence of a cytosolic unilocular lipid vesicle. These lipid droplets account for up to 95% of the volume of adipocytes and push the nucleus into the periphery of the cells (Fig. 2C). Accordingly, staining with sulforhodamine B shows significant protein accumulation only at the periphery of the cells (Fig. 2B).

To validate our microscopy methodology and confirm the PAT adipocyte phenotype, we performed the analysis of three established mRNA markers typical of human adipocytes. As shown in Fig. 3A, mRNA analysis revealed a remarkable expression of PPAR γ , perilipin-1 (PLIN-1) and adiponectin (APN). Conversely, cells from the SVF obtained from the same donors showed negligible expression of these markers when compared to PAT adipocytes. To gain further insight into the expression of adipocyte markers, we performed a comparative gene expression analysis between PAT and SAT adipocytes isolated from the same donor. As shown in Fig. 3B, and as previously shown in the comparative EAT versus SAT analysis, the expression of APN was higher in SAT adipocytes

than in PAT adipocytes [26], while the expression of PPAR γ was higher in PAT adipocytes than in SAT adipocytes, contrary to our expectation [27]. Finally, no significant differences in perilipin-1 gene expression were detected between the two adipose tissue sources.

To determine whether subculturing conditions of PAT adipocytes leads to dedifferentiation process we analyzed the mRNA levels of PPAR γ and APN after 72 h from the isolation. As shown in Fig. 3B, for both PAT and SAT adipocytes we observed a slight but significant down-regulation of PPAR γ and APN expression. However, even after 72 h we found that PAT adipocytes continue to express PPAR γ and APN thousands of times more than SVF cells (data not shown) to indicate the persistence of an adipocyte phenotype.

Overall, these results indicate that prolonged subculturing can lead to a slight reduction in gene expression featuring the adipocyte phenotype. However, as will be shown in paragraph 3.3 this doesn't affect the ability of PAT adipocytes to respond to inflammatory and lipolytic stimuli.

3.2. PAT derived adipocytes viability over time and in response to various challenges

Our isolation method is aimed at obtaining a cardiac adipocyte cell model, with the dual purpose of advancing our understanding of cardiac fat pathophysiology and providing a valuable platform for screening new therapeutics. Therefore, central to our study is the evaluation of cell vitality over time. To this end, we monitored cell viability up to 72 h by exposing PAT adipocytes to various pathophysiologic stimuli relevant to metabolic syndrome and inflammation and using different vitality monitoring methods: MTT, evaluation of total protein content and flow cytometry in the presence of the fluorochromes 7-AAD. As depicted in

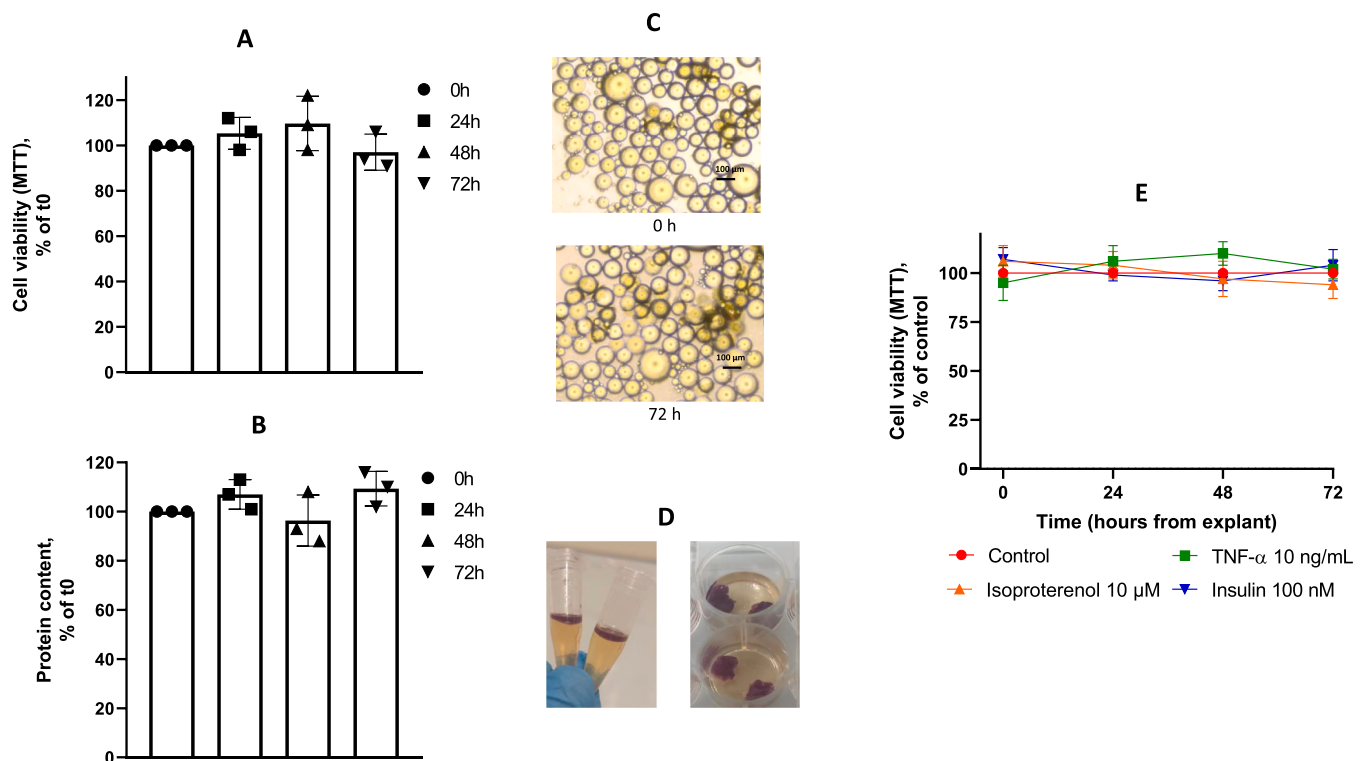


Fig. 4. PAT adipocytes cell viability over time. (A-B) PAT adipocytes viability was assessed after 0–72 h from the isolation by a 3-(4,5-dimethylthiazol-2-yl)-2,5-diphenyl tetrazolium bromide (MTT) assay (A) and by cells protein content (B). Data (means \pm S.D., $n = 3$ for each experimental condition) are expressed as percentage of isolated adipocytes at time 0. Statistical analysis was performed with one-way ANOVA followed by Bonferroni's post-hoc test. (C, D) Photographs of MTT stained PAT adipocytes and organ culture, 0 and 72 h after the isolation. (E) Effect of different stimuli on PAT adipocytes viability. Adipocytes were treated or left untreated, at different times after the isolation, with 10 ng/mL TNF- α , 10 μ M/L isoproterenol and 100 nmol/L insulin for 18 h. Cell viability was assessed by a 3-(4,5-dimethylthiazol-2-yl)-2,5-diphenyl tetrazolium bromide (MTT) assay, and data (means \pm S.D., $n = 3$ for each experimental condition) expressed as a percentage of the unstimulated control. Statistical analysis was performed with one-way ANOVA followed by Bonferroni's post-hoc test.

Fig. 4, cell vitality remained consistent over the course of 72 h, as evaluated through MTT assays (A, B) and protein content analysis (C). Moreover, there were no apparent alterations in cell morphology, indicating that the adopted experimental conditions did not adversely affect cellular integrity or viability (Fig. 4 D). It is noteworthy that over a 72-h period, cell vitality remains relatively stable, even in the presence of pathophysiological agents such as insulin, the master regulator of glucose metabolism, the pro-inflammatory cytokine TNF- α , and the lipolytic agent isoproterenol (Fig. 4 D). These findings suggest that PAT adipocytes serve as a robust and enduring cellular model, ideal for prolonged in vitro studies.

Cytofluorimetric analysis of the isolated cells showed, in agreement to previous reports [28,29] a spiral-like population on the forward scatter (FSC) and side scatter (SSC) plot. Approximately 16% of this population responded positively to staining with Nile red, indicating the presence of a substantial proportion of free lipid droplets and a minor portion of adipocytes at the top of the spiral-like population (Fig. 5 A). This distribution corresponds to the expected spatial arrangement of events in the FSC/SSC diagram, reflecting the size and internal

complexity of the cells: smaller lipid droplets with simpler structures are located in the lower part of the diagram, while larger adipocytes with more complex structures appear in the upper part (Fig. 5 A). Re-analysis using 7-AAD staining confirms that the method used to isolate the PAT adipocytes does not affect their viability, as the cell death rate under these conditions was around 9% (Fig. 5 B). To demonstrate that our protocol exclusively isolates adipocytes, we also stained both the floating cells and the stromal vascular fraction (SVF) cells, including MSCs, with the stem cell marker CD90. As shown in Fig. 5 C, cells corresponding to the adipocyte fraction do not express CD90, whereas MSCs isolated from the same tissue show high levels of this surface marker (Fig. 5 D).

3.3. Responsivity of PAT adipocyte and PAT organ culture to inflammatory and lipolytic stimuli

During obesity, cytokines from the TNF family orchestrate inflammation in adipose tissue, culminating in lipid overflow, glucotoxicity, and insulin resistance [30]. Consequently, an effective adipose cell

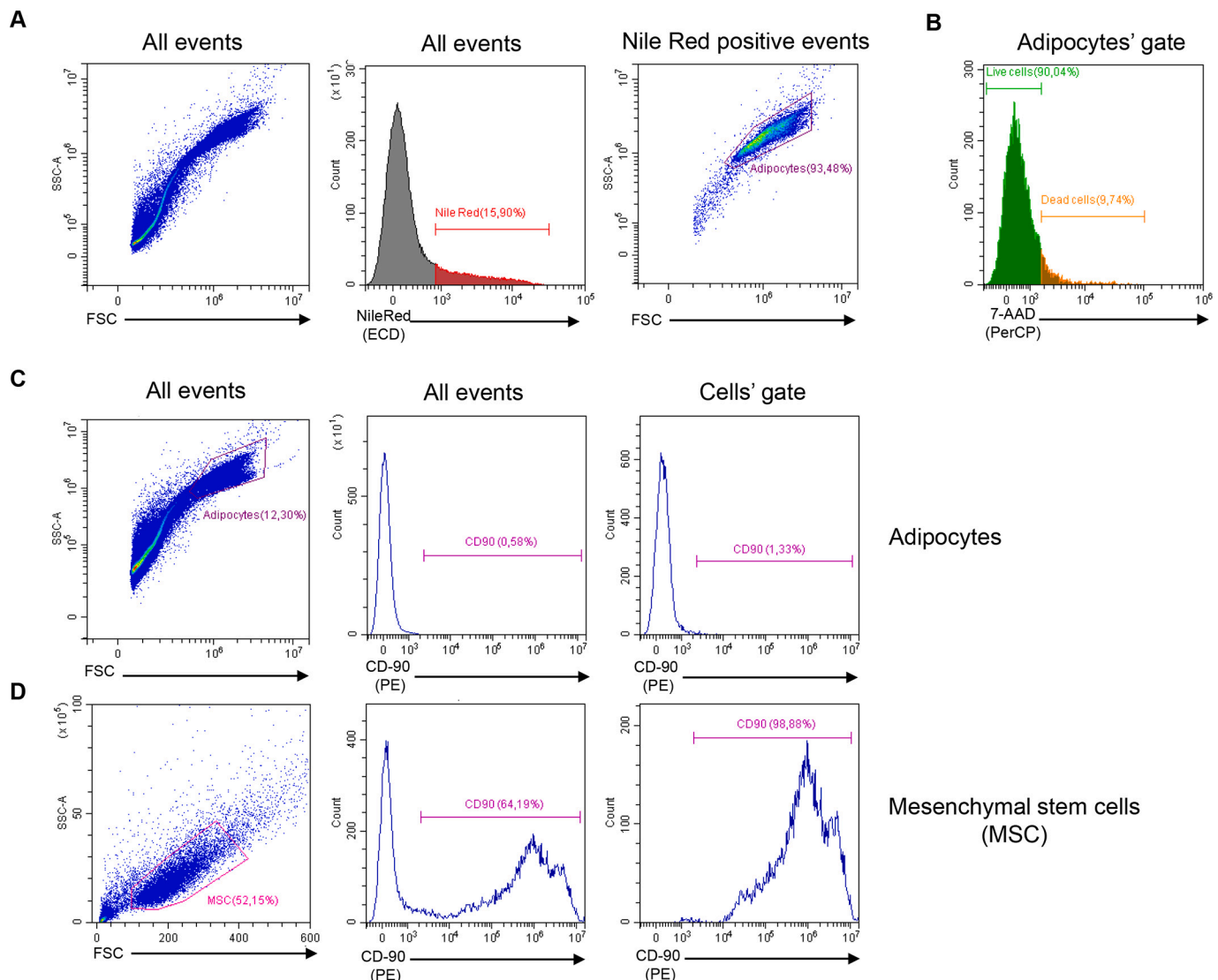


Fig. 5. Cytofluorimetric determination of cell viability. (A) Density plot of cells isolated from PAT. Adipocytes, identified by their positivity to Nile Red staining, are located on the top of the spiral-like population. (B) Histogram of adipocytes stained with 7-AAD. Histogram of adipocytes (C) and MSC (D) stained with anti-CD90 antibody: on the left is shown the percentage of CD90 positive cells over all events, at the right is shown the percentage of CD90 positive cells over the gate of cells on morphology dot plot. Data presented are representative of PAT adipocytes from four different patients. (For interpretation of the references to colour in this figure legend, the reader is referred to the web version of this article.)

model should exhibit sensitivity to both pro-inflammatory and metabolic stimuli. Operating on this premise, up to 72-h post-explantation we exposed PAT adipocytes to a challenge with TNF- α and isoproterenol. As illustrated in Fig. 5A-E, PAT adipocytes demonstrate sustained responsiveness to TNF- α , evidenced by the upregulation of various pro-inflammatory genes such as MCP-1, IL-6, and COX-2, alongside the downregulation of metabolic genes PPAR γ and APN. Notably, no significant differences were reported in the extent of the response to cytokine stimulation between adipocytes treated at the time of explantation and after 72 h. Concurrently, exposure to isoproterenol significantly stimulates glycerol release and the liberation of free fatty acids. Remarkably, this sensitivity persists, with no significant differences, for up to 72 h post-explantation (Fig. 5 F). After demonstrating the viability of the PAT organ culture, we similarly examined the responsiveness of the whole tissue to inflammatory stimuli. After 24 h in culture, we stimulated PAT with 10 ng/ml TNF- α for 5 h. As shown in Fig. 6, cytokine stimulation significantly induced the expression of MCP-1, IL-6 and TNF- α .

3.4. The pro-inflammatory secretome of PAT derived adipocytes and PAT organ culture alters the phenotype and function of endothelial cells

Subclinical inflammation in the arteries is considered a major factor in the development of atherosclerosis and associated clinical complications even in subclinical atherosclerosis [31]. Previous investigations have emphasized the significant involvement of visceral adipose tissue including EAT in this intricate process apparently driven by the adipose-mediated release of pro-inflammatory cytokine and exosomes [32–34]. We were therefore prompted to evaluate and confirm the pro-

inflammatory and pro-atherosclerotic role of PAT and PAT-derived adipocytes. Recognizing the endothelium as a pivotal cellular entity in orchestrating atherosclerosis [35], we chose to assess the effect of PAT

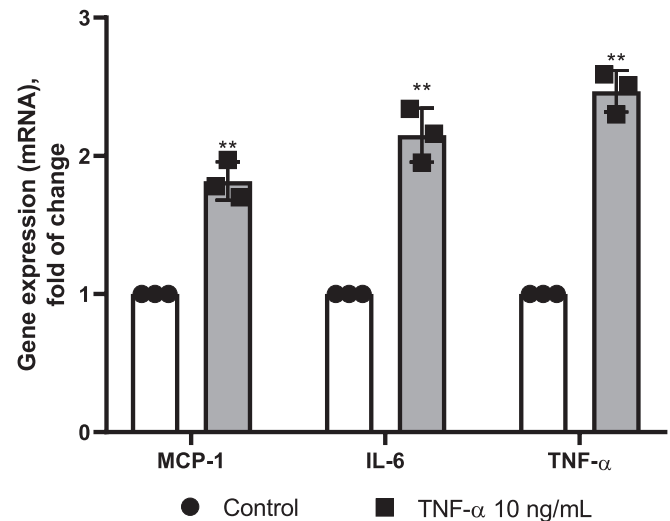


Fig. 7. TNF- α induces inflammation in PAT organ culture. PAT pieces were placed in culture and treated with 10 ng/mL TNF- α for 18 h or left untreated. The mRNA levels of MCP-1, IL-6 and TNF- α were measured by qPCR using specific primers and normalized to β -actin mRNA. Data (mean \pm S.D., n = 3 for each experimental condition) are expressed as fold-induction versus untreated control. Statistical analysis was performed with Student's t-test. **p < 0.01.

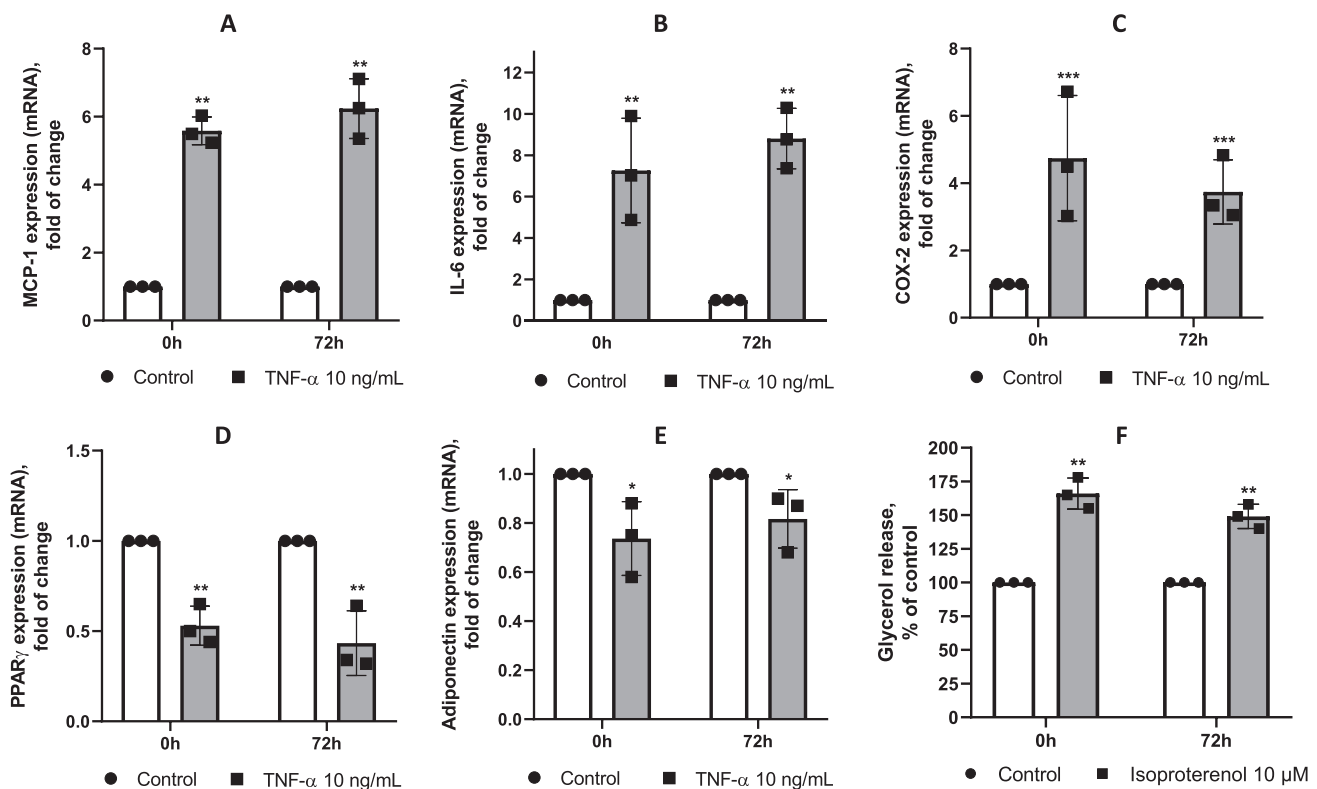


Fig. 6. PAT adipocytes respond to inflammatory stimuli 72 h after explantation. (A-E) PAT adipocytes were treated or left untreated with 10 ng/mL TNF- α for 5 h at different time points after isolation. The mRNA levels of MCP-1, IL-6, COX-2, PPAR γ and adiponectin were measured by qPCR using specific primers and normalized to β -actin mRNA. Data (mean \pm S.D., n = 3 for each experimental group and condition) are expressed as fold-induction versus untreated control. Statistical analysis was performed with Student's t-test. *p < 0.05; **p < 0.01; ***p < 0.001. (F) PAT adipocytes were treated or left untreated, at different times after the isolation, with 10 μ M/L isoproterenol for 24 h. Culture media were collected and total amount of released glycerol was measured as an index of lipolysis. Data (means \pm S.D., n = 3 for each experimental group and condition) are expressed as percent of untreated control. Statistical analysis was performed with Student's t-test. **p < 0.01.

secretome on endothelial phenotype and function. As shown in Fig. 7, the exposure of human endothelial cells to conditioned media from PAT and PAT-derived adipocytes, though to a lesser extent than exogenous TNF- α , induced a substantial gene reprogramming. This was evidenced by the endothelial upregulation of pro-inflammatory and plaque-destabilizing genes, including MCP-1, COX-2, and MMP-9, and notably, the endothelial leukocyte adhesion molecule VCAM-1. Consistent with the upregulation of VCAM-1, endothelial cells exposed OCM exhibited a significant increase in monocyte adhesion to the endothelial monolayer ($130\% \pm 25$ for PAT CM vs. $210\% \pm 18$ for TNF- α , respectively; $p < 0.01$). (See Fig. 8.)

3.5. Pat adipocytes and MSC fatty acid composition

Considering that the FA composition of adipose tissue, including EAT, has been recognized for several years as a durable biomarker providing insights into both dietary habits and fatty acid metabolism [36–39], we decided to also investigate the FA composition of PAT adipocytes.

After 48 h in culture, our study, as shown in Fig. 9, indicates a marked predominance of oleic acid and monounsaturated fatty acids (MUFAs), over both saturated and unsaturated fats. This pattern was also observed in MSC from paired donors. Notably, MSC displayed relatively higher levels of linoleic, arachidonic, and docosahexaenoic acids compared to PAT adipocytes. The fatty acid profile of PAT adipocytes closely mirrors the patterns reported in PAT tissue by Hjelmgaard [40]. Among polyunsaturated fatty acids (PUFAs), n-6 were more abundant than n-3, with only a trace amount docosahexaenoic acid

detected. Additionally, we observed significant levels of palmitoleic acid (16:1n-7), which has been linked to obesity in adipose tissue [41] and associated with increased cardiovascular mortality when present in serum [42].

4. Discussions

We have developed a streamlined method for isolating mature fat cells from PAT, a cardiac fat depot easily and safely reachable during conventional cardiac surgery as well as in other different minimally invasive approaches such as partial-sternotomy or right mini-thoracotomy. Our method ensures the isolation of adipocytes that maintain their viability for up to 72 h post-explantation. These adipocytes exhibit responsiveness to various challenges, including pro-inflammatory and metabolic stimuli, demonstrating their ability to provoke a pro-inflammatory response and impact endothelial cell behavior. Simultaneously, we established conditions to sustain whole PAT in culture, preserving its viability and responsiveness to external stimuli.

It is widely acknowledged that prolonged caloric excess, coupled with low energy expenditure, results in the buildup of surplus energy in the form of triglycerides within diverse adipose tissue depots. This accumulation raises significant health concerns, especially when it involves visceral adipose tissue, such as the fat surrounding the heart or cardiac fat [43]. Cardiac fat resides in three distinct regions recognized as EAT, PAT, and as intramyocardial adipose tissues with different mesenchymal origin and vascularization. PAT comprises fat deposits located between the visceral and parietal pericardium [44]. It originates

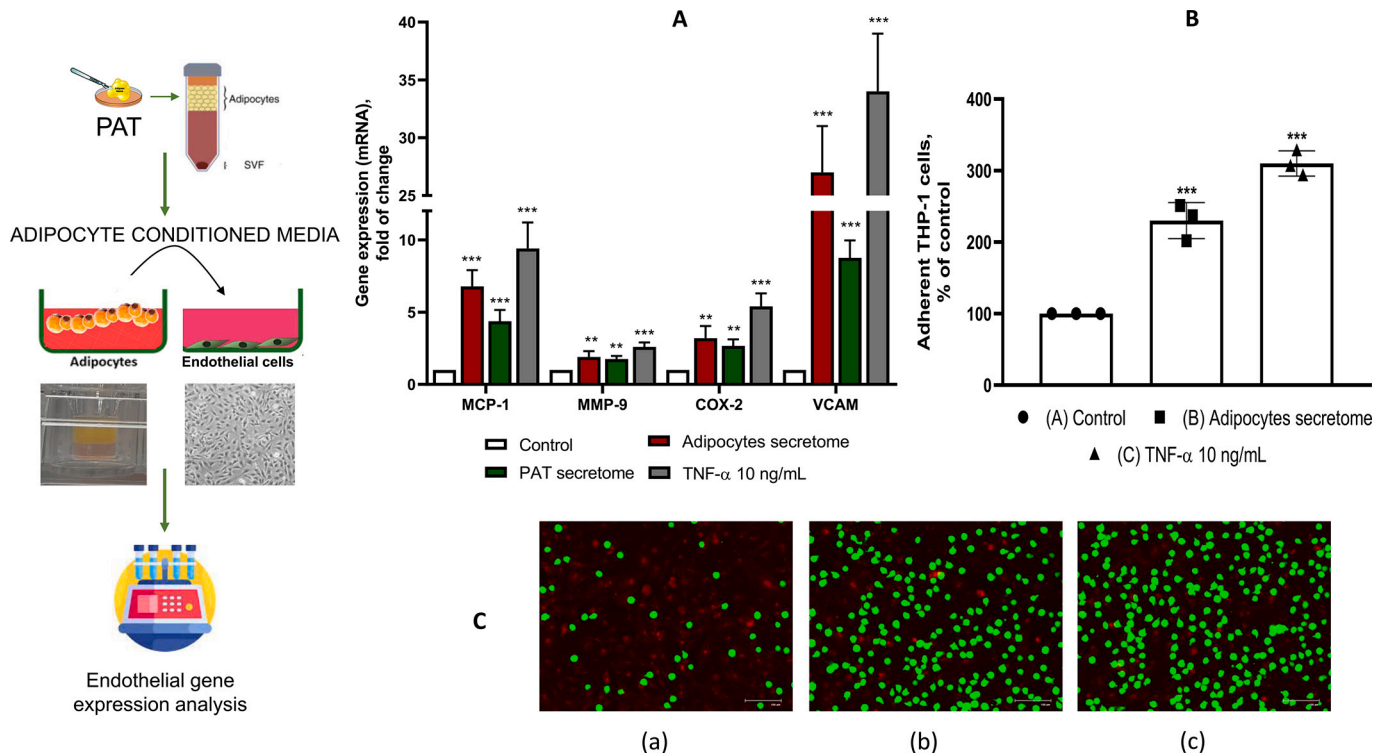


Fig. 8. The secretome of PAT and PAT adipocytes induces inflammation in human endothelial cells. PAT and PAT adipocytes were placed in a Transwell™ system, and the conditioned medium in the lower chamber was collected after 24 h and used to stimulate endothelial cells. HMEC-1 were treated with tissue and adipocyte secretion at a 1:1 ratio with MCDB-131 and with 10 ng/mL TNF- α as a positive control or left untreated for 18 h. (A) The mRNA levels of MCP-1, MMP-9, COX-2 and VCAM-1 were measured by qPCR using specific primers and normalized to GAPDH mRNA. Data (mean \pm S.D., $n = 3$ for each experimental condition) are expressed as fold-induction versus untreated control. Statistical analysis was performed with Student's t-test. ** $p < 0.01$; *** $p < 0.001$. Individual data points are listed in the supplementary table 1 (B, C) THP-1 (10^6 cells/mL) were labeled with green fluorescence using Calcein-M, then added to HMEC-1 monolayers, which were labeled with the red fluorescent dye DiI18. After 1 h, the non-adherent cells were removed by washing three times, and the images of HMEC-1 and adherent THP-1 cells were visualized and recorded using a phase-contrast microscope at $10\times$ magnification. Data (means \pm S.D., $n = 3$ for each experimental condition) are expressed as percentage of adherent monocytes compared to untreated control. Statistical analysis was performed with Student's t-test. ** $p < 0.01$; *** $p < 0.001$. (For interpretation of the references to colour in this figure legend, the reader is referred to the web version of this article.)

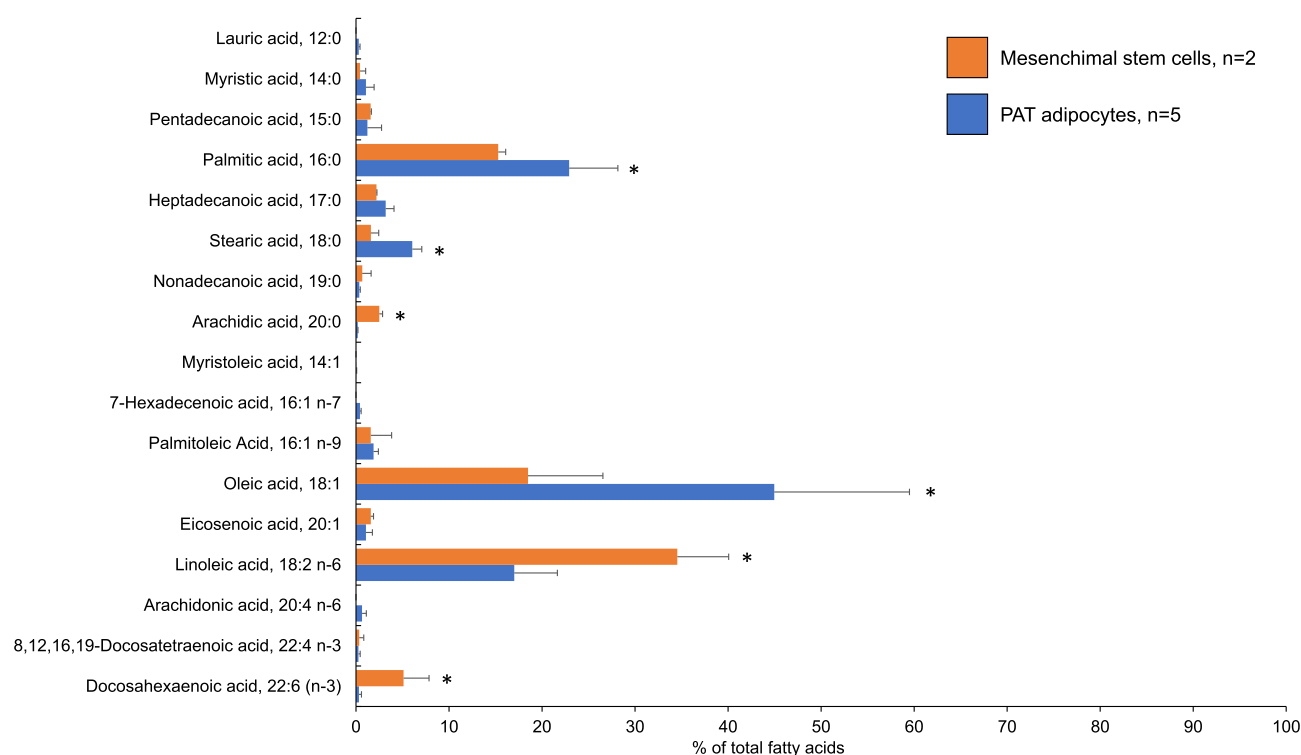


Fig. 9. Fatty acid composition (% of total FA) in PAT adipocytes and MSC. Comparison of fatty acid profiles of adipocytes and MSC isolated from PAT. Data (means \pm S.D., $n = 5$ for PAT adipocytes and $n = 2$ for MSC) are expressed as % of total fatty acids. Statistical analysis was performed with Student's t-test. * $p < 0.05$. Individual data points are listed the supplementary table 2.

from primitive thoracic mesenchyme that subsequently divides to give rise to the parietal pericardium and to the outer chest wall. The vascular supply to PAT comes from the pericardiophrenic branches of the internal mammary artery [4]. EAT originates from the splanchnopleure of the mesoderm [4]. Positioned posterior to the PAT and situated between the visceral layer of the pericardium and the heart, EAT lacks of fascia barrier from the myocardium [6]. This absence allows it to directly envelops the myocardium and coronary vessels, providing a housing for the ganglia of the cardiac nervous system and plexi. EAT shares with myocardium branches of the coronary arteries that serves as a common source for blood supply [6]. The anatomical and embryological disparities between EAT and PAT suggest the likelihood of distinct contributions to the physiopathology of the cardiovascular system [13]. However, despite these differences, both adipose depots have been correlated with the risk of heart disease, including coronary atherosclerosis, heart failure, and aortic stenosis [11,12,45,46]. This underscores the need to develop integrative cellular models to further explore the pathophysiology of various adipose tissues, including PAT, in caloric excess and to investigate the interaction between such hypertrophied cardiac adipose tissue and the cardiovascular system.

While it is widely acknowledged that the optimal cardiovascular research strategy should prioritize the human being as a whole, it is also widely recognized that, aside from the obvious ethical issues, studying the human body at both tissue and molecular levels presents challenges due to the lack of suitable study models that accurately recapitulate human cardiovascular diseases. Up to now, the majority of research efforts have been focused on investigating adipose tissue utilizing rodent models, which have revealed numerous promising therapeutic targets for addressing obesity and metabolic disorders. Nevertheless, translating these findings into clinical applications for humans has proven challenging, primarily due to substantial differences between human physiology and animal model systems [47]. Since no animal model can fully recapitulate the complexity of human atherosclerosis [47] or the physiological parameters determining intrinsic and/or acquired resistance to

cardio protective medicaments, the best approach is the use a combination of models, including patients-derived cells to gain the most insightful information on, drug metabolism, pharmacodynamics, biomarkers, nutraceutical responses prior to clinical translation [48]. Patients tissue culture systems have been in existence since the 1950s [49], but despite strong evidence for their clinical predictivity, they have not been widely incorporated into the cardiovascular drug development pipeline [50].

Being adipose tissue collection relatively non-invasive in clinical settings, the evaluation of gene expression signature of adipose depots has been shown to be of advantage for combining epidemiological and molecular aspects of biomedical research and nutrigenomics [51]. Adipose tissue explants [33,51] as well as peripheral blood mononuclear cell (PBMC) [52] may be manipulated as “organ culture” allowing researchers to study the long-term effects of exogenous stimuli including drugs and nutraceutical compounds. They offer the potential possibility to characterize patient-specific responses to therapies and provide the unique opportunity to identify novel biomarkers of response that could be used to stratify patients' risk. Furthermore, the culturing of adipose tissue explants is also relatively inexpensive compared with the production and maintenance of mouse models or the isolation and culture of organoids, which often require costly cell culture reagents and matrices for their maintenance [53].

Our patient-derived pure adipocytes and adipose tissue cultures fulfil all these requirements: they are affordable, ready to use, permanently viable, and responsive. These cultured tissues recapitulate numerous biological characteristics observed in vivo, underscoring their relevance for studying adipose tissue dynamics and responses.

In terms of lipid content, the composition of our PAT adipocytes closely resembles that found in the human PAT sample by Hjelmgaard et al. [40]. The evaluation of fatty acid composition of EAT and PAT is of great importance due to their close anatomical proximity to coronary arteries and myocardial tissue. This close relationship implies that beyond the influence of traditional adipokines, these fat depots may

influence cardiac function through the release of specific fatty acids and their metabolites, including prostaglandins, thromboxanes, leukotrienes, and lipoxins [54]. Thus, evaluation of adipocyte fatty acid profiles provides valuable insight into potential mechanisms by which EAT and PAT may contribute to cardiac health and disease. In addition, the evaluation of specific fatty acid allows conclusions to be drawn about previous dietary habits. For example, in rabbits exposed to a high-cholesterol diet, EAT was shown to be significantly enriched in saturated fatty acids at the expense of MUFAs and PUFAs [39]. Marine n-3 PUFAs, in particular, are incorporated into cell lipids and metabolised into less pro-inflammatory products than n-6 PUFAs [55]. This suggests a potential anti-inflammatory effect of n-3 PUFAs that may be of clinical importance in the context of adipose tissue [56]. It is therefore possible that a diet enriched with the cardio-protective n-3 PUFAs may lead to a favourable shift in fatty acid composition in the EAT and PAT. This hypothesis is currently being investigated in our laboratory. Also noteworthy is the presence of cis-7-hexadecenoic acid, a positional isomer of palmitoleic acid, which is significantly more abundant in PAT adipocytes than in MSCs. The analysis of 16:1n-7 in humans has often led to contradictory results. Epidemiologic studies have found a positive correlation between 16:1n-7 levels in adipose tissue and obesity [41], while its serum levels have been positively associated with cardiovascular mortality [42]. Foamy macrophage, which are key functional elements in the atherosclerotic lesion, are enriched in cis-7-hexadecenoic acid (16:1n-9) [57]. Nevertheless, research indicates that adipocyte-secreted C16:1n7 improves muscle insulin sensitivity and reduces hepatic fat accumulation [58], while in white adipocytes, it promotes lipolysis [59]. Further investigation is needed to determine whether the presence of C16:1n7 in PAT is functionally associated with lipolysis activation and whether it confers protective or detrimental effects on excessive fat accumulation.

In terms of gene expression, our study suggests that the cells retain their capacity to maintain responsive cellular signaling machineries when exposed to external stimuli. These findings are in line with those reported by Ballasy et al. in their investigation of EAT organ culture, where responsiveness to pro-diabetic stimuli was observed [33]. Our results are also in partial agreement with those of Gesta et al. [60], as we also observed a slight deregulation of basal expression of adipose-specific genes, including PPAR γ and APN, but not actin, during the 72-h culture period (data not shown). On the other hand, in close accordance with Gesta et al. [60], our results reveal no significant changes in the lipolytic activity of PAT adipocytes after 72 h. This was corroborated by the absence of any evidence of delipidation, indicating the preserving of metabolic activity and differentiation characteristics.

Although it is widely recognized that the main pro-inflammatory activity of adipose tissue originates from resident macrophages [14,61–63], our data clearly emphasize the additional pro-inflammatory contribution of PAT adipocytes. We observe that exposure of endothelial cells to the conditioned medium of PAT adipocytes leads to profound reprogramming of endothelial genes, including upregulation of MCP-1 and VCAM-1, which are functionally involved in adhesion of monocytes to the vascular endothelium in atherosclerosis [64], in addition to COX-2 and MMP-9, which are involved in plaque instability [65]. Our data are consistent with previous observations by Henrichot et al. [66] and Cejkova et al. [67] regarding the release of cytokines and the ability of adipocytes to maintain monocyte adhesion to CCM preconditioned endothelial cells.

In conclusion, our study has revisited and implemented a collagenase-mediated enzymatic method to successfully isolate viable adipocytes from cardiac fat depots. We have demonstrated the acquisition of a significant quantity of pure adipocyte cultures that remain viable and responsive for up to 72 h. By overcoming the challenges associated with accessing samples from the cardiothoracic surgery division, this method provides a functional and relatively straightforward approach to investigating the pathophysiology of obesity and cardiac dysfunction.

The efficiency in obtaining cells, coupled with the low dedifferentiation processes, suggests the potential for future applications as a personalized tool for screening and evaluating individual patient responses to drugs and nutraceuticals.

Funding

This work is supported by the European Union, “Next Generation EU” and the Italian Ministry of University and Research to MM (PRIN-2022 Prot. 2022NZNZH8) and to NC (PRIN 2022 prot. 2022CAKEW9). It was also supported by “Tecnopolo per la medicina di precisione” (TecnMed Puglia) - Regione Puglia: DGR n. 2117 del 21/11/2018, CUP: B84I18000540002” to IP

CRediT authorship contribution statement

Stefano Quarta: Writing – review & editing, Writing – original draft, Supervision, Project administration, Methodology, Investigation, Formal analysis, Data curation, Conceptualization. **Giuseppe Santarpino:** Writing – review & editing, Methodology. **Maria Annunziata Carluccio:** Writing – review & editing, Supervision, Resources, Funding acquisition. **Nadia Calabriso:** Writing – review & editing, Supervision, Methodology, Data curation. **Francesco Cardetta:** Methodology. **Laura Siracusa:** Writing – review & editing, Methodology, Investigation. **Tonia Strano:** Methodology, Investigation. **Ilaria Palamà:** Writing – review & editing, Methodology, Investigation. **Gabriella Leccese:** Writing – review & editing, Methodology, Investigation. **Francesco Visioli:** Writing – review & editing, Funding acquisition. **Marika Massaro:** Writing – review & editing, Writing – original draft, Visualization, Supervision, Resources, Project administration, Methodology, Investigation, Funding acquisition, Formal analysis, Data curation, Conceptualization.

Declaration of generative AI and AI-assisted technologies in the writing process

The authors did not use generative AI or AI-assisted technologies in the development of this manuscript.

Declaration of competing interest

None.

Appendix A. Supplementary data

Supplementary data to this article can be found online at <https://doi.org/10.1016/j.yjmcc.2024.08.006>.

References

- [1] C. Auger, S. Kajimura, Adipose tissue remodeling in pathophysiology, *Ann. Rev. Pathol.: Mech. Disease* 18 (2023) 71–93.
- [2] R.K. Zwick, C.F. Guerrero-Juarez, V. Horsley, M.V. Plikus, Anatomical, physiological, and functional diversity of adipose tissue, *Cell Metab.* 27 (2018) 68–83.
- [3] C. Li, X. Liu, B.K. Adhikari, L. Chen, W. Liu, Y. Wang, et al., The role of epicardial adipose tissue dysfunction in cardiovascular diseases: an overview of pathophysiology, evaluation, and management, *Front. Endocrinol.* 14 (2023).
- [4] M.M. Lima-Martínez, C. Blandinier, G. Iacobellis, Epicardial adipose tissue: More than a simple fat deposit?, in: *Endocrinología y Nutrición*, English edition 60, 2013, pp. 320–328.
- [5] G. Iacobellis, A.C. Bianco, Epicardial adipose tissue: emerging physiological, pathophysiological and clinical features, *Trends Endocrinol. Metab.* 22 (2011) 450–457.
- [6] B. Gaborit, C. Sengenès, P. Ancel, A. Jacquier, A. Doutour, Role of Epicardial adipose tissue in health and disease: a matter of fat? *Compr. Physiol.* 7 (2017) 1051–1082.
- [7] Z. Lu, Z. Jiang, J. Tang, C.P. Lin, H. Zhang, Functions and origins of cardiac fat, *FEBS J.* 290 (2023) 1705–1718.
- [8] M. Koenen, M.A. Hill, P. Cohen, J.R. Sowers, Obesity, adipose tissue and vascular dysfunction, *Circ. Res.* 128 (2021) 951–968.

- [9] A.B. Engin, Adipocyte-macrophage cross-talk in obesity, *Adv. Exp. Med. Biol.* 960 (2017) 327–343.
- [10] Y. Liu, Y. Sun, C. Hu, J. Liu, A. Gao, H. Han, et al., Perivascular adipose tissue as an indication, contributor to, and therapeutic target for atherosclerosis, *Front. Physiol.* 11 (2020).
- [11] B. Chong, J. Jayabaskaran, J. Ruban, R. Goh, Y.H. Chin, G. Kong, et al., Epicardial adipose tissue assessed by computed tomography and echocardiography are associated with adverse cardiovascular outcomes: a systematic review and meta-analysis, *Circ Cardiovasc Imaging* 16 (2023) e015159.
- [12] H.K. Al-Makhamreh, A.A. Toubasi, L.M. Al-Harasis, F.H. Albustanji, T.N. Al-Sayegh, S.M. Al-Harasis, Pericardial fat and cardiovascular diseases: a systematic review and meta-analysis, *J. Evid. Based Med.* 16 (2023) 178–185.
- [13] G. Iacobellis, Epicardial and pericardial fat: close, but very different, *Obesity* 17 (2009) 625.
- [14] E. Ortega Martinez de Victoria, X. Xu, J. Koska, A.M. Francisco, M. Scalise, A. W. Ferrante Jr., et al., Macrophage content in subcutaneous adipose tissue: associations with adiposity, age, inflammatory markers, and whole-body insulin action in healthy Pima Indians, *Diabetes* 58 (2009) 385–393.
- [15] R. Madonna, M. Massaro, E. Scoditti, I. Pescetelli, R. De Caterina, The epicardial adipose tissue and the coronary arteries: dangerous liaisons, *Cardiovasc. Res.* 115 (2019) 1013–1025.
- [16] M. Greif, A. Becker, F. von Ziegler, C. Leberher, M. Lehrke, U.C. Broedl, et al., Pericardial adipose tissue determined by dual source CT is a risk factor for coronary atherosclerosis, *Arterioscler. Thromb. Vasc. Biol.* 29 (2009) 781–786.
- [17] G.A. Rodriguez-Granillo, E. Reynoso, C. Capunay, J. Carpio, P. Carrascosa, Pericardial and visceral, but not total body fat, are related to global coronary and extra-coronary atherosclerotic plaque burden, *Int. J. Cardiol.* 260 (2018) 204–210.
- [18] Y. Si, Z. Cui, J. Liu, Z. Ding, C. Han, R. Wang, et al., Pericardial adipose tissue is an independent risk factor of coronary artery disease and is associated with risk factors of coronary artery disease, *J. Int Med Res* 48 (2020) 300060520926737.
- [19] World Medical Association Declaration of Helsinki, Recommendations guiding physicians in biomedical research involving human subjects, *JAMA* 277 (1997) 925–926.
- [20] H. Sugihara, N. Yonemitsu, S. Miyabara, K. Yun, Primary cultures of unilocular fat cells: characteristics of growth in vitro and changes in differentiation properties, *Differentiation* 31 (1986) 42–49.
- [21] P. Greenspan, E.P. Mayer, S.D. Fowler, Nile red: a selective fluorescent stain for intracellular lipid droplets, *J. Cell Biol.* 100 (1985) 965–973.
- [22] IUPAC, Preparation of Fatty Acid Methyl Ester, in *Standard Methods for Analysis of Oils, Fats and Derivatives*, Blackwell, Oxford, 1987.
- [23] E.G. Bligh, W.J. Dyer, A rapid method of total lipid extraction and purification, *Can. J. Biochem. Physiol.* 37 (1959) 911–917.
- [24] M. Massaro, G. Basta, G. Lazzarini, M.A. Carluccio, F. Bosetti, G. Solaini, et al., Quenching of intracellular ROS generation as a mechanism for oleate-induced reduction of endothelial activation and early atherogenesis, *Thromb. Haemost.* 88 (2002) 335–344.
- [25] J. Panes, M. Perry, D.N. Granger, Leukocyte-endothelial cell adhesion: avenues for therapeutic intervention, *Br. J. Pharmacol.* 126 (1999) 537–550.
- [26] C. Bambace, A. Sepe, E. Zoico, M. Telesca, D. Olivos, S. Venturi, et al., Inflammatory profile in subcutaneous and epicardial adipose tissue in men with and without diabetes, *Heart Vessel.* 29 (2014) 42–48.
- [27] B. Gaborit, N. Venticlef, P. Ancel, V. Pelloux, V. Gariboldi, P. Leprince, et al., Human epicardial adipose tissue has a specific transcriptomic signature depending on its anatomical peri-atrial, peri-ventricular, or peri-coronary location, *Cardiovasc. Res.* 108 (2015) 62–73.
- [28] C.E. Hagberg, Q. Li, M. Kutschke, D. Bhowmick, E. Kiss, I.G. Shabalina, et al., Flow cytometry of mouse and human adipocytes for the analysis of Browning and Cellular heterogeneity, *Cell Rep.* 24 (2018), 2746–2756 e5.
- [29] B.B. Boumelhem, S.J. Assinder, K.S. Bell-Anderson, S.T. Fraser, Flow cytometric single cell analysis reveals heterogeneity between adipose depots, *Adipocyte* 6 (2017) 112–123.
- [30] X. Hildebrandt, M. Ibrahim, N. Peltzer, Cell death and inflammation during obesity: “know my methods, WAT(son)”, *Cell Death Differ.* 30 (2023) 279–292.
- [31] L. Fernández-Friera, V. Fuster, B. López-Melgar, B. Oliva, J. Sánchez-González, A. Macías, et al., Vascular inflammation in subclinical atherosclerosis detected by hybrid PET/MRI, *J. Am. Coll. Cardiol.* 73 (2019) 1371–1382.
- [32] N. Alexopoulos, D. Katsitsis, P. Raggi, Visceral adipose tissue as a source of inflammation and promoter of atherosclerosis, *Atherosclerosis* 233 (2014) 104–112.
- [33] N.N. Ballasy, A.S. Jadli, P. Edalat, S. Kang, A. Fatehi Hassanabad, K.P. Gomes, et al., Potential role of epicardial adipose tissue in coronary artery endothelial cell dysfunction in type 2 diabetes, *FASEB J.* 35 (2021) e21878.
- [34] R. Mei, W. Qin, Y. Zheng, Z. Wan, L. Liu, Role of adipose tissue derived exosomes in metabolic disease, *Front. Endocrinol. (Lausanne)* 13 (2022) 873865.
- [35] S.R. Botts, J.E. Fish, K.L. Howe, Dysfunctional vascular endothelium as a driver of atherosclerosis: emerging insights into pathogenesis and treatment, *Front. Pharmacol.* 12 (2021) 787541.
- [36] A.C. Beynen, R.J. Hermus, J.G. Hautvast, A mathematical relationship between the fatty acid composition of the diet and that of the adipose tissue in man, *Am. J. Clin. Nutr.* 33 (1980) 81–85.
- [37] L. Arab, J. Akbar, Biomarkers and the measurement of fatty acids, *Public Health Nutr.* 5 (2002) 865–871.
- [38] L. Hodson, C.M. Skeaff, B.A. Fielding, Fatty acid composition of adipose tissue and blood in humans and its use as a biomarker of dietary intake, *Prog. Lipid Res.* 47 (2008) 348–380.
- [39] M. Pezeshkian, M.R. Rashidi, M. Varmazyar, J. Hanaee, A. Darbin, M. Nouri, Influence of a high cholesterol regime on epicardial and subcutaneous adipose tissue fatty acids profile in rabbits, *Metab. Syndr. Relat. Disord.* 9 (2011) 403–409.
- [40] K. Hjelmgaard, R.B. Eschen, E.B. Schmidt, J.J. Andreasen, S. Lundbye-Christensen, Fatty acid composition in various types of cardiac adipose tissues and its relation to the fatty acid content of atrial tissue, *Nutrients* 10 (2018).
- [41] J. Gong, H. Campos, S. McGarvey, Z. Wu, R. Goldberg, A. Baylin, Adipose tissue palmitoleic acid and obesity in humans: does it behave as a lipokine? *Am. J. Clin. Nutr.* 93 (2011) 186–191.
- [42] E. Warensjö, J. Sundström, B. Vessby, T. Cederholm, U. Risérus, Markers of dietary fat quality and fatty acid desaturation as predictors of total and cardiovascular mortality: a population-based prospective study, *Am. J. Clin. Nutr.* 88 (2008) 203–209.
- [43] N. González, Z. Moreno-Villegas, A. González-Bris, J. Egido, Ó. Lorenzo, Regulation of visceral and epicardial adipose tissue for preventing cardiovascular injuries associated to obesity and diabetes, *Cardiovasc. Diabetol.* 16 (2017) 44.
- [44] L. Chhabra, N. Gurukripa Kowligi, Cardiac adipose tissue: distinction between epicardial and pericardial fat remains important!, *Int. J. Cardiol.* 201 (2015) 274–275.
- [45] S. Kenchaiah, J. Ding, J.J. Carr, M.A. Allison, M.J. Budoff, R.P. Tracy, et al., Pericardial fat and the risk of heart failure, *J. Am. Coll. Cardiol.* 77 (2021) 2638–2652.
- [46] S. Quarta, G. Santarpino, M.A. Carluccio, N. Calabriso, M. Maffia, L. Siculella, et al., Exploring the significance of epicardial adipose tissue in aortic valve stenosis and left ventricular remodeling: unveiling novel therapeutic and prognostic markers of disease, *Vasc. Pharmacol.* 152 (2023) 107210.
- [47] J. Seok, H.S. Warren, A.G. Cuenca, M.N. Mindrinos, H.V. Baker, W.H. Xu, et al., Genomic responses in mouse models poorly mimic human inflammatory diseases, *P Natl Acad Sci USA* 110 (2013) 3507–3512.
- [48] W. Hu, C. Jiang, D. Guan, P. Dierickx, R. Zhang, A. Moscati, et al., Patient adipose stem cell-derived adipocytes reveal genetic variation that predicts antidiabetic drug response, *Cell Stem Cell* 24 (2019), 299–308.e6.
- [49] R.A. Vertrees, J.M. Jordan, T. Solley, T.J. Goodwin, Tissue culture models, *Basic Conc. Mol. Pathol.* 2 (2009) 159–182.
- [50] M. Lippi, I. Stadiotti, G. Pompilio, E. Sommariva, Human cell modeling for cardiovascular diseases, *Int. J. Mol. Sci.* 21 (2020).
- [51] E. Diaz-Rodriguez, R.M. Agra, A.L. Fernandez, B. Adrio, T. Garcia-Caballero, J. R. Gonzalez-Juanatey, et al., Effects of dapagliflozin on human epicardial adipose tissue: modulation of insulin resistance, inflammatory chemokine production, and differentiation ability, *Cardiovasc. Res.* 114 (2018) 336–346.
- [52] A. Camargo, P. Pena-Orihuela, O.A. Rangel-Zuniga, P. Perez-Martinez, J. Delgado-Lista, C. Cruz-Teno, et al., Peripheral blood mononuclear cells as in vivo model for dietary intervention induced systemic oxidative stress, *Food Chem. Toxicol.* 72 (2014) 178–186.
- [53] I.R. Powley, M. Patel, G. Miles, H. Pringle, L. Howells, A. Thomas, et al., Patient-derived explants (PDEs) as a powerful preclinical platform for anti-cancer drug and biomarker discovery, *Br. J. Cancer* 122 (2020) 735–744.
- [54] M. Masoodi, O. Kuda, M. Rossmeisl, P. Flachs, J. Kopecky, Lipid signaling in adipose tissue: Connecting inflammation & metabolism, *Biochim. Biophys. Acta (BBA) - Mol. Cell Biol. Lipids* 1851 (2015) 503–518.
- [55] R. De Caterina, n-3 fatty acids in cardiovascular disease, *N. Engl. J. Med.* 364 (2011) 2439–2450.
- [56] S. Chiusolo, C.S. Bork, F. Gentile, S. Lundbye-Christensen, W.S. Harris, E. B. Schmidt, et al., Adipose tissue n-3/n-6 fatty acids ratios versus n-3 fatty acids fractions as predictors of myocardial infarction, *Am. Heart J.* 262 (2023) 38–48.
- [57] C. Guijas, C. Meana, A.M. Astudillo, M.A. Balboa, J. Balsinde, Foamy monocytes are enriched in cis-7-Hexadecenoic fatty acid (16:1n-9), a possible biomarker for early detection of cardiovascular disease, *Cell. Chem. Biol.* 23 (2016) 689–699.
- [58] H. Cao, K. Gerhold, J.R. Mayers, M.M. Wiest, S.M. Watkins, G.S. Hotamisligil, Identification of a lipokine, a lipid hormone linking adipose tissue to systemic metabolism, *Cell* 134 (2008) 933–944.
- [59] A. Bolsoni-Lopes, W.T. Festuccia, T.S. Farias, P. Chimim, F.L. Torres-Leal, P. B. Derogis, et al., Palmitoleic acid (n-7) increases white adipocyte lipolysis and lipase content in a PPARalpha-dependent manner, *Am. J. Physiol. Endocrinol. Metab.* 305 (2013). E1093–102.
- [60] S. Gesta, K. Lolmede, D. Daviaud, M. Berlan, A. Bouloumié, M. Lafontan, et al., Culture of human adipose tissue explants leads to profound alteration of adipocyte gene expression, *Horm. Metab. Res.* 35 (2003) 158–163.
- [61] S.P. Weisberg, D. McCann, M. Desai, M. Rosenbaum, R.L. Leibel, A.W. Ferrante Jr., Obesity is associated with macrophage accumulation in adipose tissue, *J. Clin. Invest.* 112 (2003) 1796–1808.
- [62] R. Yu, C.S. Kim, B.S. Kwon, T. Kawada, Mesenteric adipose tissue-derived monocyte chemoattractant protein-1 plays a crucial role in adipose tissue macrophage migration and activation in obese mice, *Obesity (Silver Spring)* 14 (2006) 1353–1362.
- [63] C. Pang, Z. Gao, J. Yin, J. Zhang, W. Jia, J. Ye, Macrophage infiltration into adipose tissue may promote angiogenesis for adipose tissue remodeling in obesity, *Am. J. Physiol. Endocrinol. Metab.* 295 (2008) E313–E322.
- [64] J.R. Pickett, Y. Wu, L.F. Zacchi, H.T. Ta, Targeting endothelial vascular cell adhesion molecule-1 in atherosclerosis: drug discovery and development of vascular cell adhesion molecule-1-directed novel therapeutics, *Cardiovasc. Res.* 119 (2023) 2278–2293.
- [65] D. Sef, M. Kovacevic, B. Jernej, K. Novacic, M. Slavica, J. Petrak, et al., Immunohistochemical analysis of MMP-9 and COX-2 expression in carotid

- atherosclerotic plaques among patients undergoing carotid endarterectomy: a prospective study, *J. Stroke Cerebrovasc. Dis.* 31 (2022) 106731.
- [66] E. Henrichot, C.E. Juge-Aubry, A. Pernin, J.C. Pache, V. Velebit, J.M. Dayer, et al., Production of chemokines by perivascular adipose tissue: a role in the pathogenesis of atherosclerosis? *Arterioscler. Thromb. Vasc. Biol.* 25 (2005) 2594–2599.
- [67] S. Cejkova, H. Kubatova, F. Thieme, L. Janousek, J. Fronek, R. Poledne, et al., The effect of cytokines produced by human adipose tissue on monocyte adhesion to the endothelium, *Cell Adhes. Migr.* 13 (2019) 293–302.